JOURNAL OF MATERIALS SCIENCE: MATERIALS IN MEDICINE **16** (2005) 739–744

Macroporous calcium phosphate glass-ceramic prepared by two-step pressing technique and using sucrose as a pore former

CONG WANG, TOSHIHIRO KASUGA, MASAYUKI NOGAMI
Graduate School of Engineering, Nagoya Institute of Technology, Gokiso-Cho, Showa-Ku, Nagoya 466-8555, Japan

Macroporous calcium phosphate glass-ceramic with an initial glass composition of $60CaO{\cdot}30P_2O_5{\cdot}3TiO_2{\cdot}7Na_2O$ in mol% was successfully prepared by sintering the mixture compact consisting of calcium phosphate glass and sucrose powders, which was formed using a two-step pressing technique. After burning off the sucrose phase, a 3D interconnected macroporous structure was formed in the sintered body, in which the skeleton consisting of the calcium phosphate glass-ceramic (including β-calcium pyrophosphate and β-tricalcium phosphate as the crystalline phases) was transformed from the initial glass during the sintering. The macropores with several hundred microns in diameter and the large interconnection size ($\sim$100 μm), which result from the controllably large-sized sucrose particles and the hot-pressing at a little higher temperature than the sucrose's melting point, are believed to meet the requirements for cell adhesion and bone tissue regeneration well. Moreover, *in vitro* dissolution behavior study indicates that the calcium phosphate glass-ceramic is soluble to an acetic acid solution of pH 5–7. These, together with the simplicity and feasibility of the innovative fabrication method itself, show that the formed porous glass-ceramic has a promising potential for application to a scaffold for bone tissue engineering.

1. Introduction

With the development of surgical technique and medical knowledge, there is an increasing demand for synthetic bone-graft substitutes, resulting from the limited supply of autograft materials. Among them, calcium-phosphate-based biomaterials have received considerable attention, primarily because of their excellent biocompatibility and bone regeneration properties, as well as close similarity in composition with nature bone [1], and they have been widely used in low-load-bearing applications [2, 3]. In dentistry, they are used for the augmentation of deficient mandibular of maxillar ridges, and in orthopedic surgery, for filling bone defects. In addition, they have also been investigated for the delivery of drugs, marrow and cultured marrow cells.

Synthesizing or regenerating tissues and organs is a main task of tissue engineering. Recently, this has been done by providing a synthetic porous scaffold to mimic the body's own extracellular matrix, onto which cells attach, proliferate, differentiate and organize. In bone tissue engineering, the calcium-phosphate-based scaffolds are accepted to use as a carrier or template for implanted bone cells or other growth factors for the formation of bone from the surrounding tissue [4]. On the other hand, to serve as a scaffold it should exhibit appropriate spatial and appropriate compositional properties. High porosity is necessary for supporting the adhesion of a large number of cells, whereas high pore interconnectivity can enable cell suspensions to penetrate the structure, promote the transport of nutrients and waste products, and thus to encourage tissue ingrowth. These pore characteristics are essential for cell attachment, proliferation and differentiation. A minimum pore size of approximately 100–150 μm has been established as necessary for the continued health of bony ingrowth [1, 5, 6]. However, some research groups have suggested that the degree of interconnectivity is more critical than the pore size [7–9]. In addition, the skeleton properties, such as biocompatibility, rate of degradation and mechanical attributes during the bone growth and remodeling, are the key factors that determine whether a scaffold is suitable for a particular application [10, 11].

Some techniques for fabrication of porous HA scaffolds have been developed, such as replication of a polymer sponge, incorporation of volatile organic particles, etc. [12, 13], since HA has been evidenced its long-term biocompatibility and its favorable interaction with soft tissue and bone in many vivo studies [14]. However a modification of these methods is still expected and necessary, because the method of the incorporation

of volatile organic particles easily results in a porous structure of closed and poorly interconnected [15–17], whereas the polymer sponge method usually exhibits a poor mechanical strength due to the existence of numerous micropores within the skeletons, although it can produce an open pore system with a controllable pore size, interconnected pores and desired geometry [18–22].

Recently we have developed a silica-free calcium phosphate glass-ceramic with an mother glass composition of $60CaO{\cdot}30P_2O_5{\cdot}3TiO_2{\cdot}7Na_2O$ (in mol%), which showed excellent biocompatibility and bioactivity as well as good mechanical properties in our previous studies [23–27]. Particularly the apatite-forming ability of it in simulated body fluid (SBF, at 37 °C) has been drastically enhanced after autoclaving at 140 °C for 1 h, and the apatite began to appear on the surfaces of autoclaved glass-ceramic after only 3 days of soaking and could cover the surfaces completely within 10 days [28]. Consequently, if a macroporous material of this glass-ceramic can be prepared, it will have a promising potential for application to the bone tissue engineering. In the present work, a two-step pressing technique for forming was adopted, and with the aid of controllably large-sized sucrose particles and the second step hot-pressing, we successfully prepared calcium phosphate glass-ceramic with a 3D interconnected macroporous structure. It is believed that this simple and innovative fabrication process is also effective and feasible for the formation of macroporous ceramics or other inorganic materials.

2. Experimental

2.1. Mother glass preparation

Calcium phosphate invert glass with a composition of $60CaO{\cdot}30P_2O_5{\cdot}3TiO_2{\cdot}7Na_2O$ (mol%) was prepared by melting the batch in a platinum crucible at 1300 °C for 30 min. The starting raw materials, consisting of regent-grade $CaCO_3$, Na_2CO_3, TiO_2 and H_3PO_4 (85% liquid), were mixed thoroughly with a certain amount of water and then dried for the next melting process. The melt after melting at 1300 °C for 30 min in a platinum crucible was poured onto a stainless-steel plate directly and suffered a quick pressing by using an iron plate to form glass plates with the thickness of 0.5–1.0 mm. In this study, two kinds of particle sizes of glass were employed for preparation of porous glass-ceramics. One came from the as-resulting glass which was crushed and ground by a mortar and a pestle, and then sieved by using a sieve of 125 μm to control the particle size smaller than 125 μm (the mean particle size is approximately 15–20 μm), and the other from the above obtained glass particles with a further wet-grinding in a ball mill for 2 days, giving out the mean particle size of approximately 1–5 μm. In this case, the average particle size is obviously smaller than that of the former one without ball milling. Herein these two kinds of particle size are briefed as LSP (for large-sized particles, without ball-milling) and SSP (for small-sized particles, with ball-milling), respectively.

2.2. Fabrication of macroporous glass-ceramics

Calcium phosphate glass-ceramic with a 3D interconnected macroporous structure was fabricated by incorporating sucrose (Nacalai Tesque Inc., Japan, <500 μm) into initial calcium phosphate glass particles and by using a two-step pressing technique. The well-mixed particles (a small amount of PVA binder (8 wt%) was added, and the sucrose/glass ratios were controlled as 1.5:1 and 1:1 in wt, respectively) were placed into a stainless steel die and then uniaxially pressed at 15–20 MPa to form an initial compact. After the initial compact with the die was heated to 170 °C for 1 h, it was hot-pressed again around the temperature by the pressure of 15–20 MPa. Finally, the green compact obtained by the two-step pressing process was fired at a heating rate of 1.2 °C/min to an elevated temperature (800–850 °C for large-sized particles, 780–850 °C for small-sized particles) for burning off the sucrose phase and forming the macroporous glass-ceramics. The duration time for heat treatment was in the range of 0–5 h, and then the sample was free cooling down inside the furnace. A schematic representation for the whole fabrication process is illustrated in Fig. 1. X-ray diffraction patterns showed that the glass-ceramics include crystalline phases such as β-calcium pyrophosphate and β-tricalcium phosphate.

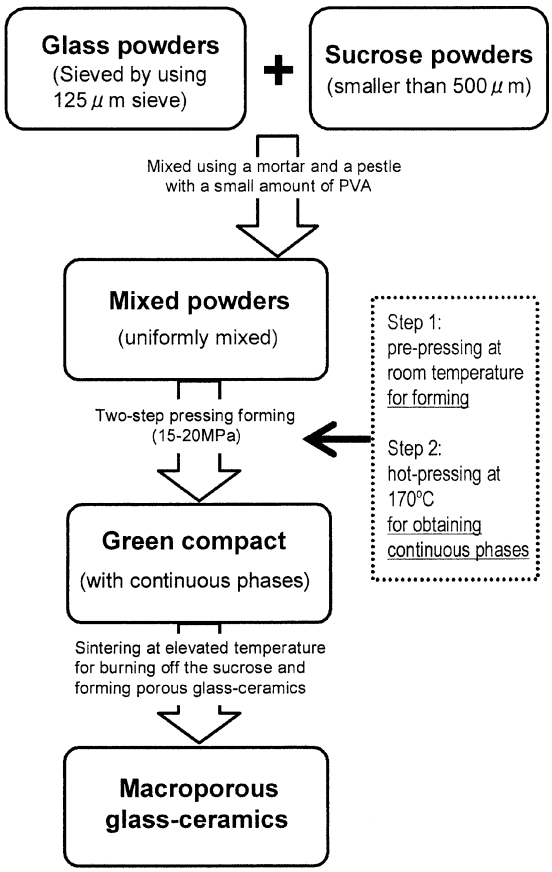

Figure 1 Schematic process for macroporous calcium phosphate glass-ceramics formation.

2.3. Characteristics of the formed macroporous glass-ceramics

The pore characteristic of the prepared macroporous glass-ceramics, such as pore size, pore interconnection and other microstructure information, was observed using field emission scanning electron microscope (FE-SEM, JEOL JSM6301F, Japan). Apparent density of the porous glass-ceramic was determined by mass-dimension evaluation, and then compared with the real density of the glass (measured by a pycnometer method) to give out an approximate porosity of the formed porous glass-ceramic. Highly interconnected porous structure and macropores could be easily achieved by our established method, i.e., by incorporating sucrose as a pore former and using two-step pressing technique. The effect of some important factors on pore characteristics, such as starting particle size of glass and heat treatment conditions, was studied and discussed.

2.4. Evaluation of the dissolution behavior of glass-ceramics

In vitro dissolution behavior of the glass-ceramic was investigated by soaking its particles in an acetic acid solution at 37 °C (with an initial pH value of 5.0) and then analyzed by an inductively coupled plasma atomic emission spectroscopic analyzer (ICP-AES, Shimadzu, ICPS-500, Japan). In order to understand its relative resorbability, the pure hydroxyapatite (HA) ceramic (sintered at 1100 °C for 3 h) was simultaneously selected to study at the same conditions for comparison. 200 mg of the glass-ceramic particles (53–125 μm) was rapidly introduced into 100 ml above acetic acid solution for a pre-determined time. The solution with glass-ceramic particles was stirred continuously throughout the experiment, then it was separated by filtration and 30 ml of withdrawn solution was analyzed with ICP-AES to obtain the solution compositions, which were further evaluated through the use of chemical potential plots (the ion activity was estimated using a Davis' equation: $\log f_i = -Az^2\{sq(\mu)/(1+sq(\mu)) - sq(\mu)\}$; where f_i: ion activity, μ: ionic strength, z: electrovalence, A: constant) for understanding the resorbability of glass-ceramic [29].

3. Results and discussion

3.1. Formation of interconnected macroporous structure

In this study, the two-step pressing technique was employed to fabricate macroporous glass-ceramics, in which sucrose was used as a pore former. Fig. 2 shows the typical porous structures of our samples with different particle sizes (Fig. 2(a) for the sample formed by LSP and Fig. 2(b) for the sample formed by SSP), prepared by the two-step pressing method. Obviously, for both of the samples the formed pores in the structure are mainly spherical macropores (several hundred microns in diameter), and they are evenly distributed throughout the sample. The structural characteristics of the samples are three dimensionally interpenetrating network of skeletons and pores. Undoubtedly, the

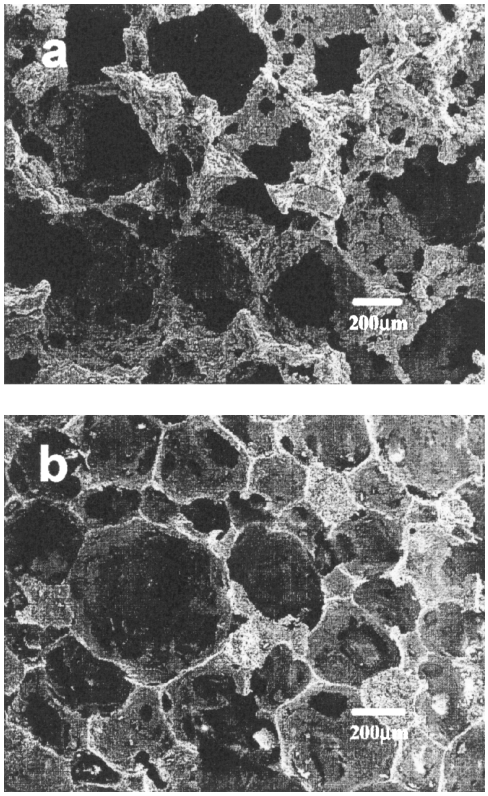

Figure 2 SEM photographs of the macroporous calcium phosphate glass-ceramic (sucrose/glass ratio is 1.5). (a) formed by LSP (heat-treated at 850 °C, 1 h) and (b) formed by SSP (heat-treated at 790 °C, 1 h).

achievement of 3D interconnected macroporous structure is attributed to the innovative method. Thanks to the sucrose particles begin to melt at 160 °C, the second step pressing, i.e., the hot-pressing at around 170 °C, makes the sucrose phase in the green compact become a continuous phase, leading to a final interconnected porous structure after burning off the sucrose phase, while reasonably large-sized sucrose particles should be responsible for the macropore formation.

Hulbert *et al*. [30] suggested that the optimum pore size for osteoconduction is 150 μm, and Flatley *et al*. [31] reported that a pore size of 500 μm is compatible for osteoconduction. In any case, the pore size should be controlled within a certain range (usually several hundred microns), which depends on the applied cell size and the specific surface area for the availability of binding sites. In our case, the sizes of most pores are within the range of 30–600 μm, and mainly in 100–500 μm (see Fig. 2(a), the porosity is ca.77%), which is believed to fall in an effective and desirable range, and the major interconnection size is larger than 100 μm, favoring cell adhesion and bone tissue regeneration as well as allowing biomolecules and degraded substances to freely flow into and out the scaffold [32].

3.2. Effect of glass particle size and heat treatment on porous structure

As mentioned in Section 2.1, two kinds of starting particle size of glass were employed in this study, i.e., the one without ball milling but sieved by using a sieve of 125 μm (LSP), and the one with wet ball milling

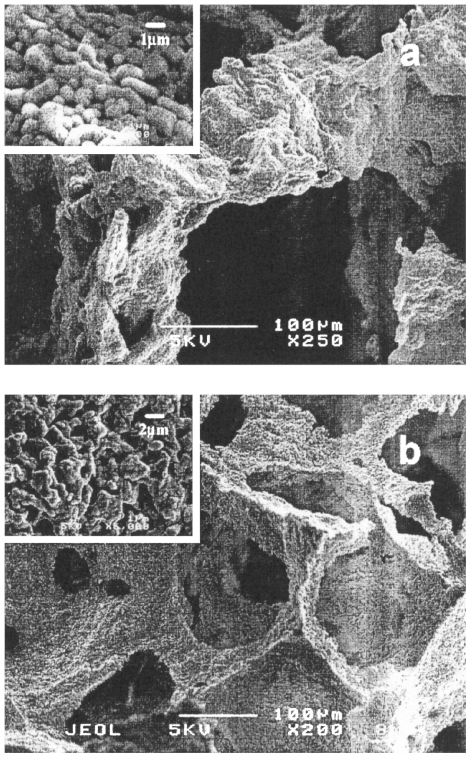

Figure 3 SEM photographs of the strut of samples (sucrose/glass ratio is 1.5). (a) formed by LSP (heat-treated at 850 °C, 1 h), (b) formed by SSP (heat-treated at 790 °C, 1 h). The insets are the higher magnification of the strut surface.

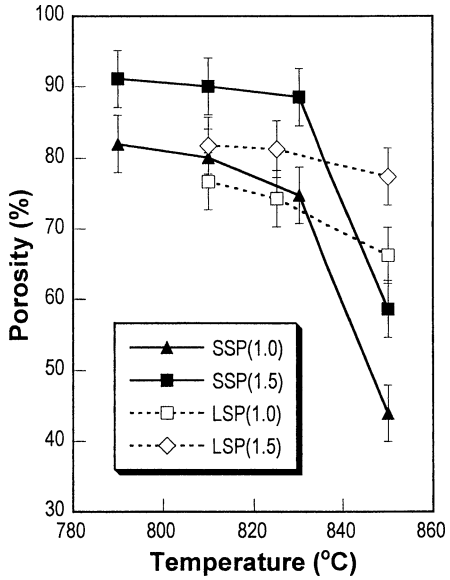

Figure 4 The variation of porosity with sintering temperature, sucrose/glass ratios and starting particle size of glass (LSP: large-sized particles, SSP: small-sized particles, and the numeral in the brackets means sucrose/glass ratio). The dwell time at different temperatures for all the samples is one hour.

for 2 days (SSP). The typical porous structures formed by using these two kinds of particles have been shown in Fig. 2. As SEM photographs shown, the skeleton wall of the sample, formed by using LSP, is thicker and seems much stronger than those formed by SSP (comparing Fig. 2(a) with Fig. 2(b)). In addition, when sintering takes place at lower than 830 °C, the porosity of LSP-formed sample usually is lower than that for SSP-formed sample, and the maximum porosity difference can be as high as 10% suppose other conditions are kept the same. These differences (in skeleton wall thickness and porosity) can seriously affect the mechanical strength of the final products. In our case, for example, most LSP-formed samples could be reasonably handled by using a pair of tweezers, however it is difficult for SSP-formed samples due to their thinner skeleton wall and too high porosity. Note that the thinner skeleton walls can also cause a collapsed pore structure easily for the SSP-formed sample during sintering at higher than 830 °C, leading to a rapid porosity decrease (will be shown a little later in Fig. 4) and non-spherical pores. Fig. 3 further shows the skeleton microstructures for the samples, formed by large- and small-sized glass particles respectively. It demonstrates that micropores can be easily remained in the skeletons for the sintered sample, formed by SSP (see Fig. 3(b)). However, for LSP-formed sample, a relatively dense skeleton can be obtained under present condition used (see Fig. 3(a)). This should be another reason responding to a poor mechanical strength of SSP-formed sample, compared with the corresponding LSP-formed sample.

The porosity of final products could be varied over a broad range via a control on heat treatment conditions and sucrose/glass ratio, and the porosity can reach up to ∼80% for the LSP-formed sample and ∼90% for the SSP-formed sample, respectively. The variation of porosity with sintering temperature, sucrose/glass ratios and starting particle size of glass are illustrated in Fig. 4. Obviously, these different factors have an evident effect on the porosity of final formed glass-ceramic, i.e., lower sintering temperature, higher sucrose/glass ratio and smaller starting particle size benefit the achievement of high porosity. It is well known that high porosity means a high surface area/volume ratio, which favors cell adhesion to the scaffold and promotes bone tissue regeneration. Although highly porous structure can be obtained by sintering at lower temperature, the mechanical strength of the solid usually is unexpected since numerous micropores still remained within the skeleton due to the insufficient sintering, especially for the sample formed by SSP (see Fig. 3(b)). As abovementioned, usage of small-sized particles easily leads to the formation of thinner skeleton walls and micropores in skeletons, thus to a poor mechanical strength. The effect of heating rate and duration time on the porosity for the sample formed by LSP is illustrated in Fig. 5. As these variable factors are chosen, there is a balance between porosity and mechanical properties, which mainly depends on the application occasion.

The porous glass-ceramic formed using LSP can be reasonably handled. From the results in Fig. 4, the apparent correlation between sucrose concentrations, starting particle sizes of glass or heat treatment conditions and the achieved porosity level suggests that it is possible to reasonably pretailor a porous glass-ceramic with a desirable porosity.

3.3. *In vitro* dissolution behaviors

Fig. 6 shows element concentrations in the acetic acid solutions (with an initial pH value of 5.0) of

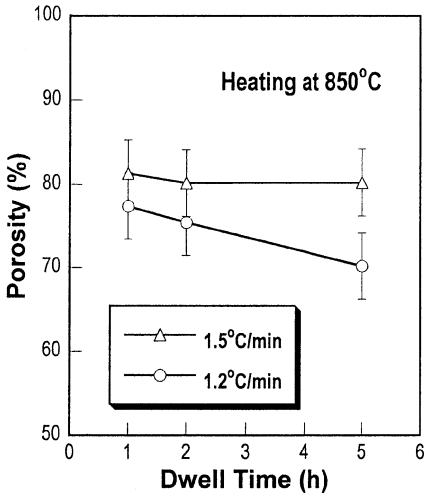

Figure 5 The effect of heating rate and dwell time on the porosity for the sample formed by LSP (sucrose/glass ratio is 1.5).

glass-ceramic and HA ceramic as a function of soaking time. As expected, the concentrations of Ca, P and Na elements in solution of glass-ceramic sample (see curve a, b and c in Fig. 6) increase gradually with the time within the measuring range, resulting from the continuous dissolution of glass-ceramic (within the soaking time, the pH value steeply increased from the initial value of 5.0 immediately ($\leq$60 min) to $\sim$7.0 for HA and $\sim$7.5 for glass-ceramic and then become approximately stable). However, this continuous dissolution behavior was not evident for Ca and P concentrations in HA ceramic sample (see curve d and e in Fig. 6, the decrease of P concentration for HA ceramic sample may result from the formation of some new calcium phosphate solids, which needs a further confirmation), which is consistent with the common idea that the dissolution of HA ceramic is quite low. This may result from an easy equilibrium with the solid sintered HA after a rapid initial concentration increase during first 30 min. Further, according to the variation of solution compositions with soaking time and the Davis' equation, the chemical potential plots for both samples were

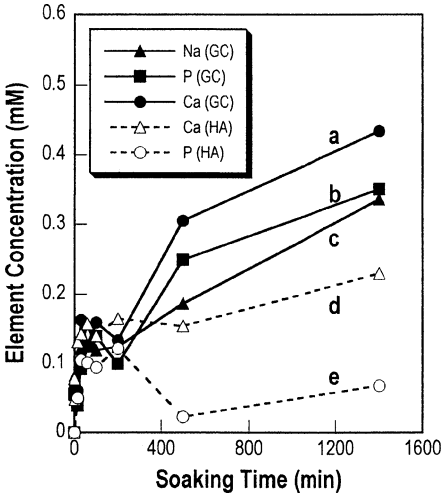

Figure 6 Variation of element concentrations after soaking the glass-ceramic and sintered HA particles in an acetic acid solution (the initial pH was adjusted to be 5.0; GC: glass-ceramic; HA: hydroxyapatite).

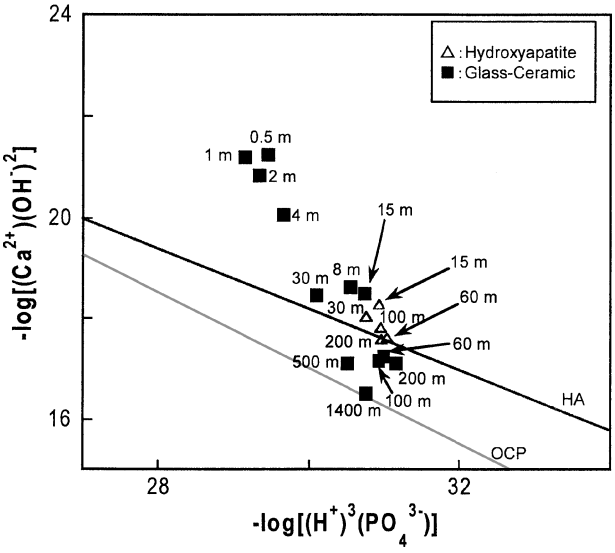

Figure 7 Chemical potential plots of the solution composition in the dissolution reactions for the glass-ceramic and sintered HA samples. (m: minute; the lines in the figure are solubility lines for hydroxyapatite (HA) and octacalcium phosphate (OCP), respectively).

analyzed and illustrated in Fig. 7. Strictly speaking, numerous ion pairs between Na^+, H^+, Ca^{2+}, OH^- and PO_4^{3-} ions should be considered. But, in the present work, to roughly estimate the chemical potential in the solution, in which the glass-ceramic was soaked, they were not considered, since the Na_2O content in the sample was very small. The straight lines in the figure are solubility lines for hydroxyapatite (HA) and octacalcium phosphate (OCP), respectively (the area above the solubility line represents the unsaturated state for the corresponding solid, and below the line it means the supersaturated area). It demonstrates that the variation of solution compositions with soaking time for glass-ceramic can occur in a wider range, compared with that for HA ceramic. It moves with the time toward the HA solubility line, then falls below this line after 60 min of soaking and moves toward the OCP solubility line, which implies that the glass-ceramic still doesn't equilibrate with the solid sintered HA under the present conditions used. Whereas the variation of solution compositions with soaking time for HA ceramic stops at a position around HA solubility line, indicating that HA ceramic sample reaches the equilibrium with solid sintered HA easily. Evidently, the above-mentioned results suggest that the resorbability of glass-ceramic is better than that of HA ceramic, which should be attributed to the existence of sodium element in glass-ceramic solution that may weaken or lower the forming ability of some calcium phosphate solids, resulting in a better solubility.

4. Conclusions

With the aid of two-step pressing technique and using sucrose as a pore former, a novel bioresorbable calcium phosphate glass-ceramic with a 3D interconnected macroporous structure was successfully obtained by sintering sucrose and glass mixed compact at an appropriate temperature. The achieved porosity of glass-ceramic can be high, and the formed macropores

(several hundred microns) and the major interconnection (>100 μm) are believed to meet the requirements for cell adhesion and bone tissue regeneration. Moreover, the porosity is closely related to the heat treatment condition, starting particle size of glass and incorporated sucrose amount, and it can be adjusted by these factors that may finally decide whether the mechanical strength of porous glass-ceramic meets the requirements for biomedical application. The study of *in vitro* dissolution behavior indicates that this glass-ceramic has a better solubility, compared with that of HA ceramic. All these achievements reveal that the obtained macroporous glass-ceramic is a potential candidate for application in bone tissue engineering, used as a scaffold. Evaluation of osteoinductivity using the glass-ceramic incorporating osteoblast cells is now in preparation.

Acknowledgments

The authors would like to acknowledge the Nagoya Institute of Technology for financial support by a grant from the NITECH 21st Century COE Program "World Ceramics Center for Environmental Harmony," and a Grant-in-Aid for Scientific Research from Japan Society for the Promotion of Science. Thanks are also due to M. Sasaki for assistance with the in vitro dissolution behavior measurements.

References

1. L. L. HENCH and J. WILSON, "An Introduction to Bioceramics" (World Scientific, London, U.K., 1993).
2. L. L. HENCH, *J. Am. Ceram. Soc.* **74**(7) (1991) 1487.
3. H. DE GROOT, *Ceram. Int.* **19** (1993) 363.
4. C. A. VACANTI and L. J. BONASSAR, *Clin. Orthop.* **367**(Suppl) (1999) S375.
5. J. J. KLAWITTER and S. F. HULBERT, *J. Biomed. Mater. Res.* **5** (1971) 161.
6. A. RAVAGLIOLI and A. KREJEWSKI, "Bioceramics: Materials, Properties, Applications" (Chapman and Hall, London, U.K., 1992).
7. J. H. KHNE, R. BARTL, B. FRISH, C. HANMER, V. JANSSON and M. ZIMMER, *Acta Orthop. Scand.* **65** (1994) 246.
8. P. S. EGGLI, W. MULLER and R. K. SCHENK, *Clin. Orthop. Rel. Res.* **232** (1998) 127.
9. R. E. HOLMES, V. MOONEY, R. BUCHOLZ and A. TENCER, *ibid.* **188** (1984) 252.
10. R. W. BUCHOLZ, A. CARLTON and R. E. HOLMES, *Orthop. Clin. North Am.* **18** (1987) 323.
11. P. A. HILL, Bone Remod., *Br. J. Orthod.* **25** (1998) 101.
12. P. SEPULVEDA, *Am. Ceram. Soc. Bull.* **76** (1997) 61.
13. J. S. WOYANSKY, C. E. SCOTT and W. P. MINNEAR, *ibid.* **71** (1992) 1674.
14. L. L. HENCH, *J. Am. Ceram. Soc.* **74** (1991) 1487.
15. O. LYCKFELDT and J. M. F. FERREIRA, *J. Eur. Ceram. Soc.* **18** (1998) 131.
16. N. O. ENGIN and A. C. TAS, *ibid.* **19** (1999) 2569.
17. *Idem.*, *J. Am. Ceram. Soc.* **83** (2000) 1581.
18. J. TIAN and J. TIAN, *J. Mater. Sci.* **12** (2001) 3061.
19. Y. ZHANG and M. ZHANG, *J. Biomed. Mater. Res.* **61** (2002) 1.
20. J. LUYTEN, J. COOYMANS, A. DE WILDE and I. THIJS, *Key Eng. Mater.* **206–213** (2002) 1937.
21. F. F. LANGE and K. T. MILLER, *Adv. Ceram. Mater.* **2** (1987) 827.
22. S. J. POWELL and J. R. G. EVANS, *Mater. Manuf. Proc.* **4** (1995) 757.
23. T. KASUGA and Y. ABE, *J. Non-Cryst. Solids* **243** (1999) 70.
24. T. KASUGA, M. SAWADA, M. NOGAMI and Y. ABE, *Biomaterials* **20** (1999) 1415.
25. T. KASUGA and Y. ABE, *J. Mater. Res.* **13** (1998) 3357.
26. T. KASUGA, M. TERADA and M. NOGAMI, *ibid.* **16** (2001) 876.
27. T. KASUGA, M. NOGAMI and M. NIINOMI, *J. Mater. Sci. Lett.* **20** (2001) 1249.
28. T. KASUGA, T. FUJIMOTO and M. NOGAMI, *J. Ceram. Soc. Jpn.* **111**(9) (2003) 633.
29. Y. DOI, T. SHIBUTANI, Y. MORIWAKI, T. KAJIMOTO and Y. IWAYAMA, *J. Biomed. Mater. Res.* **6** (1972) 347.
30. S. F. HULBERT, J. S. MORRISON and J. J. KLAWITTER, *ibid.* **39** (1998) 603.
31. T. J. FLATLEY, K. L. LYNCH and M. BENSON, *Clin. Orthop.* **179** (1983) 246.
32. P. SEPULVEDA, F. S. ORTEGA, M. D. M. INNOCENTINI and V. C. PANDOLFELLI, *J. Am. Ceram. Soc.* **83** (2000) 3021.

Received 5 March
and accepted 17 November 2004